Non-Redox-Assisted Oxygen−Oxygen Bond Homolysis in Titanocene Alkylperoxide Complexes: $[Cp_2Ti^{IV}(\eta^1\text{-}OO^tBu)L]^{+/0}$, L = Cl^-, OTf^-, Br^-, OEt_2, Et_3P

Antonio G. DiPasquale, David A. Hrovat,† and James M. Mayer*

Department of Chemistry, Campus Box 351700, University of Washington, Seattle, Washington 98195-1700

Received September 21, 2005

The titanium(IV) alkylperoxide complex $Cp_2Ti(OO^tBu)Cl$ (**1**) is formed on treatment of Cp_2TiCl_2 with $NaOO^tBu$ in THF at −20 °C. Treatment of **1** with AgOTf at −20 °C gives the triflate complex $Cp_2Ti(OO^tBu)OTf$ (**2**), which is rapidly converted to the bromide $Cp_2Ti(OO^tBu)Br$ (**3**) on addition of $^nBu_4NBr$. The X-ray crystal structures of **1** and **3** both show η^1-OO^tBu ligands. Complex **2** is stable only below −20 °C; ^1H, ^{13}C, and ^{19}F NMR spectra suggest that it also contains an η^1-OO^tBu ligand. Removal of the chloride from **1** with $[Ag(Et_2O)_2]BAr'_4$ (Ar′ = 3,5-$(CF_3)_2C_6H_3$) yields the etherate complex $[Cp_2Ti(OO^tBu)(OEt_2)]BAr'_4$ (**4**). Again, coordination of a fourth ligand to the Ti center indicates an η^1-OO^tBu ligand in **4**. These peroxide complexes do not directly oxidize olefins or phosphines. For instance, the cationic etherate complex **4** reacts with excess Et_3P simply by displacement of the ether to form $[Cp_2Ti(\eta^1\text{-}OO^tBu)(Et_3P)]BAr'_4$ (**5**). Compounds **1**−**5** all decompose by O−O bond homolysis, based on trapping and computational studies. The lack of direct oxygen atom transfer reactivity is likely due to the η^1 coordination of the peroxide and the inability to adopt more reactive η^2 geometry. DFT calculations indicate that the steric bulk of the ^{t}Bu group inhibits formation of the hypothetical $[Cp_2Ti(\eta^2\text{-}OO^tBu)]^+$ species.

Introduction

Metal peroxide complexes have been proposed as reactive intermediates in a variety of oxidation reactions ranging from industrial to biochemical processes.[1,2] Coordination of the peroxide to the metal center activates the peroxide toward direct oxidation of substrates and/or toward O−O bond cleavage to give secondary oxidants. Transition metal alkylperoxide complexes, for instance, are suggested intermediates in catalytic epoxidation reactions from the industrial production of propylene oxide to the Sharpless titanium-tartrate chiral epoxidation.[1,3,4] In biological systems, many metalloproteins are thought to utilize hydroperoxide intermediates, formed from H_2O_2 or from O_2 (+ $2e^-$ + H^+).[2] Based on these systems, many biomimetic metal systems have been developed.[1,2,5]

The oxidations of C−H bonds by metal/peroxide systems have traditionally been viewed as involving initial cleavage of the O−O bond. This can occur in either a homolytic or heterolytic manner (eqs 1, 2; Fenton/Haber-Weiss-type mechanisms).[1,6] In both cases, the peroxide cleavage is typically

$$L_nM^{n+}OOR \rightarrow L_nM^{(n+1)+}{=}O + {}^{\bullet}OR \qquad (1)$$

$$L_nM^{n+}OOR \rightarrow L_nM^{(n+2)+}{=}O + {}^{-}OR \qquad (2)$$

viewed as requiring an increase in the oxidation state of the metal center, to stabilize the resulting metal-oxo species. Newcomb and Coon have recently proposed that an iron hydroperoxide species can oxidize C−H bonds by direct OH^+ insertion without prior cleavage of the O−O bond (eq 3),[7] which has sparked new debate into metalloenzyme oxidation mechanisms.[8] An interesting feature of eq 3 is that the oxidation state

$$L_nFe^{III}OOH + R{-}H \rightarrow L_nFe^{III}O^- + ROH_2^+ \qquad (3)$$

† Department of Chemistry, University of North Texas, P.O. Box 305070, Denton, TX 76203-5070.

(1) (a) Sheldon, R. A.; Kochi, J. K. *Metal-Catalyzed Oxidation of Organic Compounds*; Academic Press: New York, 1981. (b) *Organic Peroxides*; Ando, W., Ed.; Wiley & Sons: New York, 1992. (c) *The Chemistry of Hydroxyl, Ether, and Peroxide Groups (Supplement E2)*; Patai, S., Ed.; John Wiley & Sons: New York, 1993. (d) Jones, C. W. *Applications of Hydrogen Peroxide and Derivatives*; Royal Society of Chemistry: Cambridge, 1999.

(2) (a) Solomon, E. I.; Brunold, T. C.; Davis, M. I.; Kemsley, J. N.; Lee, S.-K.; Lehnert, N.; Neese, F.; Skulan, A. J.; Yang, Y.-S.; Zhou, J. *Chem. Rev.* **2000**, *100*, 235−349. (b) Que, L., Jr.; Ho, R. Y. N. *Chem. Rev.* **1996**, *96*, 2607−2624. (c) Klinman, J. P. *Chem. Rev.* **1996**, *96*, 1−2561.

(3) Weissermel, K.; Arpe, H.-J. *Industrial Organic Chemistry*, 3rd ed.; VCH: New York, 1997; pp 240ff, 267ff.

(4) (a) Katsuki, T.; Sharpless, K. B. *J. Am. Chem. Soc.* **1980**, *102*, 5976−5978. (b) Finn, M. G.; Sharpless, K. B. *Asymmetric Synth.* **1985**, *5*, 247−308. (c) Woodard, S. S.; Finn, M. G.; Sharpless, K. B. *J. Am. Chem. Soc.* **1991**, *113*, 106−113. (d) Finn, M. G.; Sharpless, K. B. *J. Am. Chem. Soc.* **1991**, *113*, 113−126.

(5) *Biomimetic Oxidations Catalyzed by Transition Metal Complexes*; Meunier, B., Ed.; Imperial College Press, 1998.

(6) (a) Kochi, J. K. *Organometallic Mechanisms and Catalysis*; Academic: New York, 1978; Chapter 4. For a few specific examples, see: (a) Wada, A.; Ogo, S.; Nagatomo, S.; Kitagawa, T.; Watanabe, Y.; Jitsukawa, K.; Masuda, H. *Inorg. Chem.* **2002**, *41*, 616−618. (b) Que, L., Jr.; Ho, R. Y. N. *Chem. Rev.* **1996**, *96*, 2607. (c) Mahadevan, V.; Henson, M. J.; Solomon, E. I.; Stack, T. D. P. *J. Am. Chem. Soc.* **2000**, *122*, 10249−10250.

(7) (a) Newcomb, M.; Toy, P. H. *Acc. Chem. Res.* **2000**, *33*, 449−455. (b) Chandrasena, R. E. P.; Vatsis, K. P.; Coon, M. J.; Hollenberg, P. F.; Newcomb, M. *J. Am. Chem. Soc.* **2004**, *126*, 115−126. (c) Newcomb, M.; Hollenberg, P. F.; Coon, M. J. *Arch. Biochem. Biophys.* **2002**, *409*, 72−79. (d) Newcomb, M.; Shen, R.; Choi, S. Y.; Toy, P. H.; Hollenberg, P. F.; Vaz, A. D. N.; Coon, M. J. *J. Am. Chem. Soc.* **2000**, *122*, 2677−2686. (e) Toy, P. H.; Newcomb, M.; Hollenberg, P. F. *J. Am. Chem. Soc.* **1998**, *120*, 7719−7729. (f) Toy, P. H.; Newcomb, M.; Coon, M. J.; Vaz, A. D. N *J. Am. Chem. Soc.* **1998**, *120*, 9718−9719. (g) Toy, P. H.; Dhanabalasingam, B.; Newcomb, M.; Hanna, I. H.; Hollenberg, P. F. *J. Org. Chem.* **1997**, *62*, 9114−9122. (h) Coon, M. J. *Annu. Rev. Pharmacol. Toxicol.* **2005**, *45*, 1−25.

10.1021/om050818z CCC: $33.50
Publication on Web 01/21/2006

of the metal does not change. Therefore if such reactions are possible, they could occur even with nonoxidizable metal centers such as d^0 ions. d^0-Metal ions are widely used to activate peroxides but for oxygen atom transfer rather than C−H bond oxidation. The classic example is the selective epoxidation of terminal alkenes rather than oxidation of their weak allylic C−H bonds.[1,3] These reactions usually involve η^2-peroxide or η^2-alkylperoxide complexes, from which oxygen atom transfer directly gives an oxo or alkoxide complex (eq 4). η^2-Peroxide complexes are more reactive than their η^1-isomers because they are more electronically activated and more sterically accessible.[1b,c]

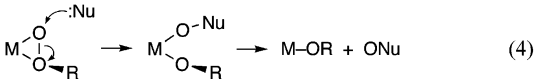

(4)

Reported in this article are the synthesis, characterization, and reactivity of new titanocene(IV) d^0 η^1-alkylperoxide complexes $Cp_2Ti(OO^tBu)L$, where L is an anionic or neutral ligand. This class of compounds was studied in order to probe the reactivity of peroxide complexes containing a nonoxidizable metal center. Related hafnium complexes $Cp^*_2Hf(OO^tBu)R$ ($Cp^* = \eta^5$-$C_5(CH_3)_5$, R = alkyl) have been reported by Bercaw and co-workers,[9] and $Cp_2Zr(OO^tBu)Cl$ has been very briefly mentioned by Schwartz and co-workers.[10,11] Titanium species have been widely used to catalyze peroxide reactions, and various intermediates have been suggested.[12] For example, the active oxidants "TiOOH" and even "Ti=O" have been proposed for reactions of titanium silicate molecular sieves using H_2O_2.[13] Homogeneous titanium/^{t}BuOOH systems epoxidize alkenes and convert sulfides into sulfoxides, in some cases with high enantiomeric excess.[4,14] Closest to the chemistry described here, Cp_2TiCl_2 is reported to catalyze the ^{t}BuOOH oxidation of bis-homoallylic alcohols into tetrahydrofuranols and tetrahydropyranols.[15] In few of these systems, however, has the reactive species been isolated and characterized in great detail.[4,14,16]

The $Cp_2Ti^{IV}(\eta^1$-$OO^tBu)L$ compounds described here are not direct oxygen atom transfer reagents toward phosphines and alkenes. Instead, they decompose at room temperature via homolysis of the peroxide bond even though formal oxidation of the metal center is not possible (eq 5). Homolytic O−O bond

$$L_nM^{n+}(OOR) \rightarrow L_nM^{n+}(O^{\bullet}) + {}^{\bullet}OR \qquad (5)$$

cleavage has previously been found in the decomposition of $Cp^*_2Hf(OO^tBu)R$ compounds.[9] The lack of reactivity of the $Cp_2Ti(\eta^1$-$OO^tBu)L$ complexes is attributed to their inability to form the more reactive and accessible η^2 conformer, even with very weakly binding ligands L. A preliminary account of part of this work has appeared.[17]

Results

I. Synthesis of $Cp_2Ti^{IV}(OO^tBu)L$ Complexes. Titanocene dichloride (Cp_2TiCl_2, $Cp = \eta^5$-C_5H_5) reacts with 4 equiv of sodium *tert*-butylperoxide ($NaOO^tBu$) in THF at −20 °C to give the new titanocene *tert*-butylperoxide complex $Cp_2Ti(OO^tBu)Cl$ (**1**) (eq 6). Low temperatures are required to prevent the

$$Cp_2TiCl_2 + NaOO^tBu \xrightarrow[-20\ ^\circ C]{THF} \underset{\mathbf{1}}{Cp_2Ti(OO^tBu)Cl} + NaCl \qquad (6)$$

decomposition of **1** as described below. Reactions using fewer than 4 equiv of $NaOO^tBu$ result in a reduced yield and starting material still present in the reaction mixture. Complex **1** is isolated in 84% yield by removal of the THF solvent and extraction with hexanes to leave unreacted $NaOO^tBu$ and NaCl behind. The yellow solid is >98% pure by ^{1}H NMR (using C_6Me_6 as an internal standard). This synthetic route follows the briefly mentioned $Cp_2Zr(OO^tBu)Cl$;[10,11] we have not been able to locate a procedure or characterization for this zirconium compound, and our attempts to produce it have not been successful (as indicated by ^{1}H NMR). The related $Cp^*_2Hf(OO^tBu)R$ was prepared by proteolysis of $Cp^*_2Hf(H)R$ with anhydrous *tert*-butylhydroperoxide.[9]

Complex **1** has been characterized by NMR, IR, and mass spectroscopies, elemental analysis, and X-ray crystallography. ^{1}H and $^{13}C\{^1H\}$ NMR spectra in THF-d_8 show the expected singlets for the Cp and ^{t}Bu groups. IR spectra in CH_2Cl_2 solutions show a moderate intensity band at 819 cm^{-1} not present in Cp_2TiCl_2 or $NaOO^tBu$, which is tentatively assigned as the O−O stretch.

Crystals of **1** suitable for X-ray diffraction were grown from a saturated toluene solution at −5 °C. Structure solution showed a typical bent-metallocene structure (Tables 1, 2; Figure 1). The *tert*-butylperoxo ligand is bound to the titanium center through only one oxygen, as indicated by the long Ti···O(2) distance of 2.952(2) Å and the open Ti−O(1)−O(2) angle of 121.5(1)°. Overall the structure is similar to that of the ethoxide analogue, $Cp_2Ti(OEt)Cl$.[18] The Ti−O(1) bond distance in **1** of 1.9090(14) Å is somewhat longer than the 1.855(2) Å Ti−OEt bond distance. The orientation of both the OO^tBu and OEt ligands has the α-substituent (O^tBu, Et) out of the equatorial plane, which allows π-donation from the oxygen p orbital to the empty $1a_1$ orbital of the $Cp_2Ti(Cl)$ metallocene fragment.[19] π-Donation

(8) (a) Auclair, K.; Hu, Z.; Little, D. M.; Ortiz de Montellano, P. R.; Groves, J. T. *J. Am. Chem. Soc.* **2002**, *124*, 6020−6027. (b) Ogliaro, F.; de Visser, S. P.; Cohen, S.; Sharma, P. K.; Shaik, S. *J. Am. Chem. Soc.* **2002**, *124*, 2806−2817. (c) Schoeneboom, J. C.; Neese, F.; Thiel, W. *J. Am. Chem. Soc.* **2005**, *127*, 5840−5853. (d) Pfister, T. D.; Ohki, T.; Ueno, T.; Hara, I.; Adachi, S.; Makino, Y.; Ueyama, N.; Lu, Y.; Watanabe, Y. *J. Biol. Chem.* **2005**, *280*, 12858−12866. (e) Cerny, M. A.; Hanzlik, R. P. *Arch. Biochem. Biophys.* **2005**, *436*, 265−275. (f) Puchkaev, A. V.; Ortiz de Montellano, P. R. *Arch. Biochem. Biophys.* **2005**, *434*, 169−177. (g) Hlavica, P. *Eur. J. Biochem.* **2004**, *271*, 4335−4360. (h) Nam, W.; Ryu, Y. O.; Song, W. J. *J. Biol. Inorg. Chem.* **2004**, *9*, 654−660. (i) Schoeneboom, J. C.; Cohen, S.; Lin, H.; Shaik, S.; Thiel, W. *J. Am. Chem. Soc.* **2004**, *126*, 4017−4034. (j) Bathelt, C. M.; Ridder, L.; Mulholland, A. J.; Harvey, J. N *J. Am. Chem. Soc.* **2003**, *125*, 15004−15005.

(9) van Asselt, A.; Santarsiero, B. D.; Bercaw, J. E. *J. Am. Chem. Soc.* **1986**, *108*, 8291−8293.

(10) Blackburn, T. F.; Labinger, J. A.; Schwartz, J. *Tetrahedron Lett.* **1975**, *35*, 3041−3044.

(11) Blackburn, T. F. Transition Metal-Assisted Oxidation of Organic Compounds. Ph.D. Thesis, Princeton University, 1977.

(12) (a) Fugiwara, M.; Wessel, H.; Hyung-Suh, P.; Roesky, H. W. *Tetrahedron* **2002**, *58*, 239−242. (b) Crocker, M.; Herold, R. H. M.; Orpen, A. G.; Overgaag, M. T. A. *J. Chem. Soc., Dalton Trans.* **1999**, 3791−3804. (c) Gallot, J. E.; Kaliaguine, S. *Can. J. Chem. Eng.* **1998**, *76*, 833−852. (d) Moller, M.; Husemann, M.; Boche, G. *J. Organomet. Chem.* **2001**, *624*, 47−52.

(13) Ratnasamy, P.; Srinivas, D.; Knoezinger, H. *Adv. Catal.* **2004**, *48*, 1−169.

(14) (a) *The Chemistry of Sulfur-containing Functional Groups*; Patai, S., Rappoport, Z., Eds.; John Wiley & Sons: New York, 1993. (b) Di Furia, F.; Licini, G.; Modena, G.; Motterle, R.; Nugent, W. A. *J. Org. Chem.* **1996**, *61*, 5175−5177. (c) Bonchio, M.; Calloni, S.; Di Furia, F.; Licini, G.; Modena, G.; Moro, S.; Nugent, W. A. *J. Am. Chem. Soc.* **1997**, *119*, 6935−6936. (d) Bonchio, M.; Licini, G.; Modena, G.; Bortolini, O.; Moro, S.; Nugent, W. A. *J. Am. Chem. Soc.* **1999**, *121*, 6258−6268.

(15) (a) Della Sala, G.; Giordano, L.; Lattanzi, A.; Proto, A.; Scettri, A. *Tetrahedron* **2000**, *56*, 3567−3573. (b) Lattanzi, A.; Della Sala, G.; Russo, M.; Scettri, A. *Synlett* **2001**, *9*, 1479−1481.

(16) Boche, G.; Möbus, K.; Harms, K.; Marsch, M. *J. Am. Chem. Soc.* **1996**, *118*, 2770−2771.

(17) DiPasquale, A. G.; Kaminsky, W.; Mayer, J. M. *J. Am. Chem. Soc.* **2002**, *124*, 14534−14535.

(18) Huffman, J. C.; Moloy, K. G.; Marsella, J. A.; Caulton, K. G. *J. Am. Chem. Soc.* **1980**, *102*, 3009−3014.

Table 1. Single-Crystal X-ray Diffraction Collection and Refinement Data for $Cp_2Ti(OO^tBu)X$

	$Cp_2Ti(OO^tBu)Cl$ (**1**)	$Cp_2Ti(OO^tBu)Br$ (**3**)
empirical formula	$C_{14}H_{19}Cl_1O_2Ti_1$	$C_{14}H_{19}Br_1O_2Ti_1$
fw	302.64	347.10
temperature (K)	130(2)	130(2)
wavelength (Å)	0.71073	0.71073
cryst description	prism	prism
color	orange	orange
cryst syst	monoclinic	monoclinic
space group	$P2_1/c$	$P2_1/c$
unit cell dimens		
a (Å)	6.4150(2)	6.6130(3)
b (Å)	12.0410(5)	11.8830(5)
c (Å)	19.0220(10)	19.0890(10)
α (deg)	90	90
β (deg)	108.7020(14)	109.0891(19)
γ (deg)	90	90
volume (Å^3)	1391.74(10)	1417.57(11)
Z	4	4
density (Mg/m^3)	1.444	1.626
abs coeff (mm^{-1})	0.798	3.414
F(000)	632	704
cryst size (mm)	0.48 × 0.26 × 0.14	0.10 × 0.10 × 0.10
no. of reflns for indexing	741	269
θ range for data collection (deg)	3.57−28.28	3.26−28.30
index ranges	$-6 \le h \le 6$ $-14 \le k \le 15$ $-25 \le l \le 25$	$-8 \le h \le 8$ $-13 \le k \le 14$ $-25 \le l \le 25$
no. of reflns collected	5103	5637
no. of unique reflns	3017	3311
R_{int}	0.0447	0.0508
completeness to $\theta = 25.00°$	96.7%	98.8%
abs corr	semiempirical	semiempirical
max./min. transmn	0.8965/0.7007	0.7265/0.7265
refinement method	full-matrix least-squares	
no. of data	3017	3311
no. of params (restraints)	166 (0)	166 (0)
goodness-of-fit on F^2 (S)	1.047	0.969
final R_1 ($I > 2\sigma$)	0.0393	0.0391
wR_2 (all data)	0.1083	0.0741
largest diff peak and hole (e/Å^3)	0.384/−0.427	0.528/−0.540

is supported by the Ti−O(1) bond distance in **1** being ∼0.1 Å shorter than that predicted for a Ti−O σ bond on the basis of covalent radii (1.99−2.05 Å[20]). This π-donation may also be the cause of the longer Ti−Cl distances in **1** and $Cp_2Ti(OEt)Cl$ (2.396(1), 2.405(1) Å) versus that in Cp_2TiCl_2 (2.364(3) Å).[21] The O(1)−O(2) distances of 1.467(2) Å in **1** and 1.489(12) Å in $Cp^*_2Hf(OO^tBu)Et$[9] are both within the range of typical peroxide bond distances (1.42 to 1.50 Å).[22] The Cl−Ti−O(1)−O(2) dihedral angle in **1** of 79.71(11)° is larger than the C(1)−Hf−O(1)−O(2) dihedral angle of 70.9(7)° in the hafnium analogue. The only other structurally characterized titanium alkylperoxide complex is an [(η^2-*tert*-butylperoxo)titanatrane]$_2$ dimer,[16] which has Ti−O(1) and O−O bond distances [1.913(3) and 1.469(3) Å] that are nearly identical to those in **1**. However, the Ti−O(2) bond distance of 2.269(2) Å and the Ti−O(1)−O(2) angle of 83.2(2)° for the η^2-peroxide are much smaller—by nearly 0.7 Å and 40°—than in the η^1-bound titanocene complex **1**.

Complex **1** reacts rapidly with 1 equiv of silver triflate (AgOTf) in THF-d_8 at −20 °C to quantitatively form the orange triflate complex $Cp_2Ti(OO^tBu)OTf$ (**2**) by ^{1}H NMR (eq 7).

$$\underset{\mathbf{1}}{Cp_2Ti(OO^tBu)Cl} + AgOTf \xrightarrow[-20\ °C]{THF} \underset{\mathbf{2}}{Cp_2Ti(OO^tBu)OTf} + AgCl \quad (7)$$

Warming solution or solid samples of **2** above 0 °C results in decomposition to black material within minutes. This instability has prevented the isolation of pure **2**. ^{1}H NMR spectra of **2** show singlets for the Cp and ^{t}Bu groups downfield from those of **1** at the same temperature. The triflate ligand is observed as a quartet at δ 120.4 ppm in the $^{13}C\{^1H\}$ NMR (J_{C-F} = 318 Hz) and as a singlet at δ 79.2 ppm by ^{19}F NMR (THF-d_8, −20 °C), similar to values for other triflate complexes.[23] ^{19}F NMR spectra of solutions containing both **2** and excess AgOTf show two signals (δ 79.2, 78.6 ppm). Since AgOTf is completely dissociated in THF,[24] this indicates that the triflate is bound to the titanium center in **2** rather than free in solution. The bound OTf^- strongly suggests that the peroxide is still η^1-bound to Ti.

Treatment of in situ-generated **2** with 1 equiv of ^{n}Bu$_4$NBr at −20 °C forms the bromide analogue of **1**, $Cp_2Ti(OO^tBu)Br$ (**3**), in 62% yield based on **1** (eq 8). The highest yields of **3** are

$$\underset{\mathbf{2}}{Cp_2Ti(OO^tBu)OTf} + {}^nBu_4NBr \xrightarrow[-20\ °C]{THF} \underset{\mathbf{3}}{Cp_2Ti(OO^tBu)Br} + {}^nBu_4NOTf \quad (8)$$

obtained when pentane and Et_2O are used as solvents for preparative reactions (THF-d_8 is used for NMR reactions) and when the solutions are kept cold throughout. Complexes **1** and **3** are isomorphous (Table 2) and have very similar spectra. The formation of **3** from **1** via **2** confirms the characterization of **2** and shows that ligand metathesis occurs readily without disruption of the *tert*-butylperoxo ligand.

To avoid the anion coordination to titanium observed for **2**, we have explored compounds with the $B[3,5\text{-}(CF_3)_2C_6H_3)]_4^-$ anion (BAr'_4^-). Reaction of **1** with 1 equiv of $AgBAr'_4{\cdot}xEt_2O$[25] in CD_2Cl_2 at −20 °C quantitatively forms the ionic species $[Cp_2Ti(OO^tBu)(OEt_2)]BAr'_4$ by ^{1}H NMR (**4**; eq 9). The coordinated

$$\underset{\mathbf{1}}{Cp_2Ti(OO^tBu)Cl} + AgBAr'_4{\cdot}xEt_2O \xrightarrow[-20\ °C]{CD_2Cl_2} \underset{\mathbf{4}}{[Cp_2Ti(OO^tBu)OEt_2]BAr'_4} + AgCl \quad (9)$$

ether in **4** [(δ 3.61 (br q, 4H), 1.29 (t, 6H)] derives from the $AgBAr'_4{\cdot}xEt_2O$; in our hands ether cannot be removed from this reagent without decomposition.[26] ^{1}H NMR spectra of reaction mixtures at −20 °C show separate Et_2O resonances

(19) Lauher, J. W.; Hoffman, R. *J. Am. Chem. Soc.* **1976**, *98*, 1729−1742.

(20) Pauling, L. *The Nature of the Chemical Bond*, 2nd ed.; Cornell University Press: New York, 1942; p 346.

(21) Clearfield, A.; Warner, D. K.; Saldarriaga-Molina, C. H.; Ropal, R.; Bernal, I. *Can. J. Chem.* **1975**, *53*, 1622−1629.

(22) Reference 1b, p 150.

(23) $^{13}C\{^1H\}$ NMR spectra and shifts for (a) AgOTf, ^{n}Bu$_4$NOTf, and TMS-OTf from: http://www.aist.go.jp/RIODB/SDBS/menu-e.html, Integrated Spectral Data Base System for Organic Compounds (accessed Mar 2005). (b) NaOTf and MeOTf from: Sigma-Aldrich Chemical Co. Web Site. http://www.sigmaaldrich.com (accessed Mar 2005).

(24) Cf. Lawrance, G. A. *Chem. Rev.* **1986**, *86*, 17−33.

(25) (a) Reger, D. L.; Wright, T. D.; Little, C. A.; Lamba, J. J. S.; Smith, M. D. *Inorg. Chem.* **2001**, *40*, 3810−3814. (b) Hayashi, Y.; Rohde, J. J.; Corey, E. J. *J. Am. Chem. Soc.* **1996**, *118*, 5502−5503.

(26) Ether-free solutions of $AgBAr^F_4$ in CH_2Cl_2 at low temperature have been described,[25b] but we were not able to prepare such solutions.

Table 2. Selected Bond Distances (Å) and Angles (deg) for $Cp_2Ti(OO^tBu)X$ (X = Cl, 1; Br, 3)[a]

	1	3		1	3
Ti−Cl/Br	2.396(1)	2.568(1)	Cp(1)−Ti−Cl/Br	105.2(2)	105.1(2)
Ti−O(1)	1.909(2)	1.922(2)	Cp(2)−Ti−Cl/Br	106.2(3)	106.2(3)
O(1)−O(2)	1.467(2)	1.472(3)	Cp(1)−Ti−Cp(2)	132.7(3)	132.7(2)
O(2)−C(11)	1.458(2)	1.457(3)	Cp(1)−Ti−O(1)	110.4(2)	110.7(3)
C(11)−C(12)	1.522(3)	1.520(4)	Cp(2)−Ti−O(1)	99.7(2)	100.0(3)
C(11)−C(13)	1.520(3)	1.522(4)	Cl/Br−Ti−O(1)	97.31(4)	96.43(7)
C(11)−C(14)	1.525(3)	1.515(4)	Ti−O(1)−O(2)	121.45(10)	120.65(14)
Cp(1)−Ti−O(1)−O(2)	29.6(2)	29.3(2)	O(1)−O(2)−C(11)	107.65(13)	107.23(19)
Cp(2)−Ti−O(1)−O(2)	172.4(3)	172.7(2)	O(2)−C(11)−C(12)	110.38(16)	110.3(2)
Cl/Br−Ti−O(1)−O(2)	79.7(3)	79.5(3)	O(2)−C(11)−C(13)	101.53(16)	101.4(2)
Ti−O(1)−O(2)-C(11)	156.6(3)	155.9(2)	O(2)−C(11)−C(14)	110.34(16)	110.6(3)

[a] Cp(#) is the centroid of the Cp ring.

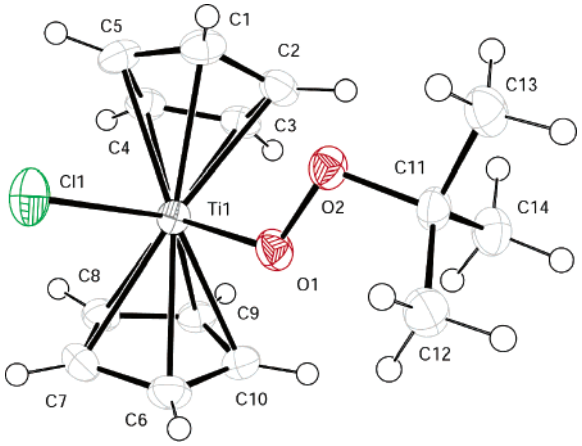

Figure 1. ORTEP diagram of $Cp_2Ti(OO^tBu)Cl$ (**1**), with thermal ellipsoids drawn at 30% probability.

for **4** and for free ether in solution. Removal of the volatiles and addition of fresh CD_2Cl_2 results in loss of the free Et_2O peaks. Exchange of bound and free Et_2O is thus slow on the NMR time scale, which is surprising since ether is typically taken as a poor ligand.[1c] The observation of a single, simple quartet for the methylene hydrogens of the bound ether indicates that there is rapid rotation about the Ti−OEt_2 bond. As found for the triflate complex **2**, binding of a weak ligand is favored over an alternative structure with an η^2-peroxide.

Generated in situ, **4** reacts with 1 equiv of Et_3P to give the phosphine complex $[Cp_2Ti(OO^tBu)(Et_3P)]BAr'_4$ (**5**, eq 10).

$$\underset{\mathbf{4}}{[Cp_2Ti(OO^tBu)OEt_2]BAr'_4} + PEt_3 \xrightarrow[-20\ ^\circ C]{CD_2Cl_2} \underset{\mathbf{5}}{[Cp_2Ti(OO^tBu)PEt_3]BAr'_4} + Et_2O \quad (10)$$

Surprisingly, no oxidation of the phosphine is seen at −20 °C by ^1H or ^{31}P NMR, even in the presence of excess PEt_3. Instead, Et_3P simply displaces the bound Et_2O. The triflate analogue of **5** is similarly formed on treatment of **2** with PEt_3. Like **2** and **4**, thermal instability in solution and in the solid state has precluded isolation of pure **5**, which has been characterized by NMR. The Cp resonance for **5** in the ^1H NMR is a doublet with $^3J_{H-P} = 3$ Hz, similar to other titanocene alkylphosphine complexes.[27] A gradient selected-HMBC 2D NMR experiment showed a correlation between the Cp ^1H NMR resonance at δ 6.27 and the ^{31}P NMR resonance at δ 27.6, confirming this assignment.

(27) (a) Van de Heisteeg, B. J. J.; Schat, G.; Akkerman, O. S.; Bickelhaupt, F. *Tetrahedron Lett.* **1987**, *51*, 6493−6496. (b) Fussing, I. M. M.; Pletcher, D.; Whitby, R. J. *J. Organomet. Chem.* **1994**, *470*, 119−125.

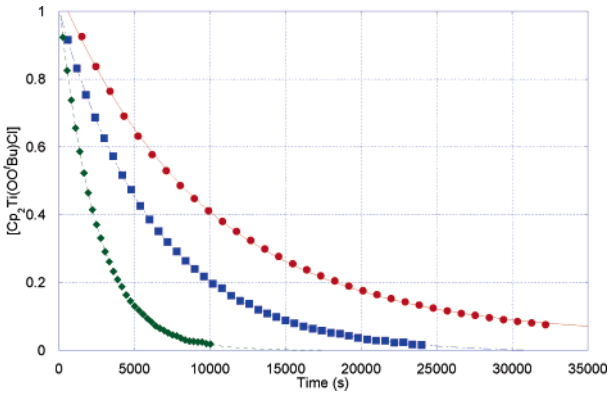

Figure 2. Plot of [**1**] versus time (using the average of both Cp and ^{t}Bu peaks from ^1H NMR) at 303 K in C_6D_{12} (●, red), C_6D_6 (■, blue), and CD_2Cl_2 (◆, green) with exponential fits.

II. Decomposition of $Cp_2Ti^{IV}(OO^tBu)L$ Complexes. All of the $Cp_2Ti^{IV}(OO^tBu)L$ complexes decompose at ambient temperatures in solution. The decompositions and all the reactions described in this account were done under anaerobic and anhydrous conditions. Complex **1** decays in CD_2Cl_2 over a couple of hours to give *tert*-butyl alcohol (96%) and a number of Cp-containing products in low yield, including Cp_2TiCl_2 (confirmed by spiking with authentic material and by mass spectrometry). Products were identified and quantified by ^1H NMR, integrating versus a C_6Me_6 internal standard. *tert*-Butyl alcohol was further confirmed by vacuum transferring the volatiles from a reaction, acquiring a ^1H NMR spectrum, and spiking the sample with ^{t}BuOH. The hydroxyl resonance of the ^{t}BuOH was not observed in any reaction mixture in either ^1H or ^2H NMR spectra, even after vacuum transfer, so it could not be determined whether the product is ^{t}BuOH or ^{t}BuOD. Other titanium products could not be identified. The *tert*-butoxide complex $Cp_2Ti(O^tBu)Cl$ is *not* among the products; it has been prepared independently from Cp_2TiCl_2 and NaO^tBu (see Supporting Information). Treatment of reaction mixtures with $HCl_{(aq)}$ or Me_3SiCl did not yield additional Cp_2TiCl_2. The decompositions of **2**−**5** in CD_2Cl_2 are quite similar to that of **1**, except that a ∼50% yield of Cp_2TiBr_2 is observed in the case of **3**.

The decompositions of **1**, **3**, **4**, and **5** in CD_2Cl_2 all follow first-order kinetics, as monitored by ^1H NMR (Figure 2; **2** has been generated only in THF). The relative rate constants fall in the order **4** > **3** ≅ **5** > **1** (Table 3). Overall, there is remarkably little variation among the four compounds, as the range in k_{dec} is less than an order of magnitude and the activation parameters are quite similar. Decomposition of **1** is slower in C_6D_{12} ($t_{1/2}$ = 2.1 h) and C_6D_6 (1.0 h) than in CD_2Cl_2 (0.5 h, Figure 2).

III. Reactivity of $Cp_2Ti^{IV}(OO^tBu)L$ Complexes. In the presence of 1 equiv of Ph_3P, the decay of **1** occurs at roughly the same rate as the decomposition of **1** (both in CD_2Cl_2; see

Table 3. Kinetic Data for the Decompositions of $Cp_2Ti^{IV}(OO^tBu)L$ in CD_2Cl_2

compound	k_{dec} (s^{-1}) (303 K)	$\Delta H^{\ddagger a}$	$\Delta S^{\ddagger b}$	$\Delta G^{\ddagger}$ (298 K)[a]	range in T[c]
$Cp_2Ti(OO^tBu)Cl$ (**1**)	$(4.1 \pm 0.2) \times 10^{-4}$	24 ± 2	5 ± 2	22 ± 2	283−313
$Cp_2Ti(OO^tBu)Br$ (**3**)	$(3.2 \pm 0.3) \times 10^{-4}$	23 ± 2	1 ± 2	22 ± 2	283−318
$Cp_2Ti(OO^tBu)(OEt_2)^+$ (**4**)	$(7.1 \pm 0.3) \times 10^{-3}$	22 ± 2	3 ± 2	21 ± 2	266−306
$Cp_2Ti(OO^tBu)(PEt_3)^+$ (**5**)	$(3.2 \pm 0.2) \times 10^{-4}$	24 ± 2	4 ± 2	23 ± 2	286−326

[a] kcal mol^{-1}. [b] cal K^{-1} mol^{-1}. [c] Temperature range (K) of rate constants used in Eyring analysis.

Table 4. Products and Rate Constants for Reactions of $Cp_2Ti(OO^tBu)Cl$ (1) in CD_2Cl_2[a]

reaction	$k \times 10^4$ (s^{-1}) (303 K)	R_3PO	R_2PO^tBu	^tBuOH[b]	$Me_2C{=}CH_2$	^tBuCl	Cp_2TiCl_2
1	4.1 ± 0.2			96%	n/o	n/o	5%
1 + 1 Ph_3P	5.9 ± 0.3	98%	n/o	24%	59%	12%	50%
1 + 5 Ph_3P	7.2 ± 0.6	96%	n/o	29%	56%	11%	48%
1 + 20 Ph_3P	6.9 ± 0.5	97%	n/o	26%	57%	11%	44%
1 + 20 $^nBu_3SnH$	2.8 ± 0.8			98%	n/o	n/d	4%
1 + 1 Ph_3P + 20 $^nBu_3SnH$	5.2 ± 0.6	23%	n/o	72%	n/o	n/d	4%
1 + 1 Et_3P	1.6 ± 0.7	n/o	~95%[c]	3%	tr	tr	27%
1 + 1 $P(OPh)_3$	3.2 ± 0.7	n/o	50%	28%	8%	3%	28%
1 + CBr_4	3.5 ± 0.5			95%	tr	tr	34%[d]

[a] n/d = not determined; n/o = not observed by ^1H or $^{31}P\{^1H\}$ NMR; tr = trace amount (<1%). [b] Hydroxyl resonance not observed in ^1H or ^2H NMR. [c] Et_2PO^tBu grows in to a maximum of 70% yield but is concurrently consumed; the yield reported is for Et_2PO^tBu plus its decomposition products.[29] [d] May contain $Cp_2TiClBr$ or Cp_2TiBr_2.

the kinetic studies below). Ph_3PO is formed in 98% yield, by ^1H and $^{31}P\{^1H\}$ NMR and by mass spectrometry. Cp_2TiCl_2 is produced in 50% yield, together with a number of other unidentified Cp-containing products. The total Cp integral in the ^1H NMR (δ 7.0−5.8) remains constant over the course of the reaction, indicating that little paramagnetic material is formed (<5%). The ^{t}Bu group in **1** is converted to ^{t}BuOH (23%), isobutylene ($CH_2{=}CMe_2$, 59%), and ^{t}BuCl (12%). These volatile products were most easily identified by vacuum transferring the volatiles to a new NMR tube, obtaining a ^1H NMR spectrum, and then spiking with authentic materials (^{t}BuCl was also confirmed by EI-MS). The product yields do not change substantially when the amount of Ph_3P is increased from 1 to 20 equiv. Complexes **2**−**5** react similarly with excess Ph_3P in CD_2Cl_2 (THF-d_8 for **2**) to give high yields of Ph_3PO. Excess PPh_3 added to solutions of **5** does not displace the PEt_3 bound to the Ti center.

In contrast, the reaction of **1** with 1 equiv of Et_3P in CD_2Cl_2 does not form any triethylphosphine oxide by $^{31}P\{^1H\}$ NMR. Instead, the major phosphorus-containing product is the phosphinite Et_2PO^tBu, identified by EI-MS and its characteristic ^{31}P chemical shift of δ 109.[28] Et_2PO^tBu was independently synthesized from Et_2PCl, ^{t}BuOH, and Et_3N, confirming the ^{31}P NMR chemical shift. The origin of this unusual product is discussed below. Et_2PO^tBu is slowly consumed as the reaction proceeds, yielding other unidentified phosphorus products.[29] The maximum observed yield of Et_2PO^tBu is 70%, at which point there is roughly a 25% yield of its apparent decay products, so **1** + PEt_3 appears to form the phosphinite quantitatively. No substantial difference is observed in the Cp region of reaction ^1H NMR spectra when compared to spectra for the decomposition of **1**. Reactions of **3** and **5** with Et_3P also give high yields of Et_2PO^tBu and its subsequent decomposition products. The decomposition of the phosphine complex **5** in the absence of added Et_3P does not form either phosphinite or phosphine oxide. Apparently the Et_3P initially present in **5** remains bound to titanium throughout decomposition.

The reaction of **1** with $^nBu_3P$ forms both $^nBu_2PO^tBu$ (78%) and $^nBu_3PO$ (19%, by ^1H NMR integration). These structural isomers are easily distinguished by $^{31}P\{^1H\}$ NMR.[30] Reaction of **1** and $(PhO)_3P$ gives the mixed phosphite $(PhO)_2P(O^tBu)$ by ^{31}P NMR and MS (50%);[31] the phosphate $(PhO)_3PO$ was not detected.

The kinetics of the phosphine reactions were monitored by ^1H NMR in CD_2Cl_2 at 303 K (Table 4). The decay of **1** in the presence of 1 equiv of Ph_3P (both 40 mM) follows first-order kinetics over 6 half-lives, with $k = (5.9 \pm 0.3) \times 10^{-4}$ s^{-1}. The first-order kinetics is surprising under these apparently second-order conditions. This k is only 44% faster than that found for decomposition of **1** at 303 K [$(4.1 \pm 0.2) \times 10^{-4}$ s^{-1}]. With 5 and 20 equiv of Ph_3P, $k = (7.2 \pm 0.6) \times 10^{-4}$ s^{-1} and $(6.9 \pm 0.5) \times 10^{-4}$ s^{-1}, which are only ~20% faster than the k observed for 1 equiv. Thus the reaction is not first-order in Ph_3P. In the presence of 1 equiv of Et_3P or $(PhO)_3P$, the first-order rate constants for decay of **1** are slower or comparable to the decomposition of **1** without added reagents: $(1.6 \pm 0.7) \times 10^{-4}$ s^{-1} [PEt_3], $(3.2 \pm 0.7) \times 10^{-4}$ s^{-1} [$(PhO)_3P$] versus $k_{dec(\mathbf{1})} = (4.1 \pm 0.2) \times 10^{-4}$ s^{-1}. In sum, while the presence of phosphine or phosphite affects the rate of decay of **1**, the dependence on [R_3P] is closer to zero-order than first-order. As discussed below, the data are consistent with rate-limiting O−O bond homolysis that does not involve the substrate. To probe the involvement of a radical chain pathway, the decomposition of **1** was examined in the presence of $^nBu_3SnH$ and CBr_4; neither had a substantial effect on the rate constant.

Added cyclohexene, norbornene, *trans*-stilbene, dimethyl sulfide, or allyl alcohol does not significantly affect the decomposition of **1**. No products of oxidation of these substrates were observed by ^1H NMR or by GC-FID. There are only slight changes in the ratios of the products of decomposition of **1**, and the rate constant for decay of **1** is essentially unchanged. Similarly, the decomposition products from the triflate complex **2** are unaffected by the presence of cyclohexene, norbornene, or *trans*-stilbene.

(28) *Phosphorus-31 NMR: principles and applications*; Gorenstein, D., Ed.; Academic Press: Orlando, 1984.

(29) The consumption of Et_2PO^tBu in reactions of Et_3P with **1** likely results from addition of $^tBuO^{\bullet}$ to Et_2PO^tBu. The apparent products of this addition appear in the ^{31}P NMR spectrum from δ 70−30 ppm, suggesting that they are phosphorus(V) oxides.

(30) $^{31}P\{^1H\}$ NMR: $^nBu_2PO^tBu$, δ 105 and $^nBu_3PO$, δ 47 (identical to that reported for $^nBu_3PO$ in $CDCl_3$: Albright, T. A.; Freeman, W. J.; Schweizer, E. E. *J. Org. Chem.* **1975**, *40*, 3437−3441).

(31) König, T.; Habicher, W. D.; Hähner, U.; Pionteck, J.; Rüger, C.; Schwetlick, K. *J. Prakt. Chem./Chem.-Ztg.* **1992**, *334*, 333−349. EI-MS-[$(PhO)_2P(O^tBu)$]: $M^+ = 290$ *m/z*.

Table 5. Calculated Gas-Phase Bond Lengths (Å) and Angles (deg) at B3LYP/6-31G*-Optimized Geometries

	$Cp_2Ti(OO^tBu)Cl$[a]	$Cp_2Ti(O^•)Cl$[b]	$Cp_2Ti(OOH)^+$	$Cp_2Ti(OOMe)^+$	$Cp_2Ti(OO^tBu)^+$
Ti−O(1)	1.880 (1.909)	1.699	1.936	1.928	1.917
Ti−O(2)	2.838 (2.952)	n/a	2.085	2.082	2.069
Ti−Cl	2.380 (2.396)	2.384	n/a	n/a	n/a
Ti−Cp(1)[c]	2.110 (2.052)	2.078	2.044	2.052	2.055
Ti−Cp(2)[c]	2.136 (2.072)	2.111	2.050	2.054	2.065
O(1)−O(2)	1.449 (1.467)	n/a	1.460	1.460	1.462
∠Ti−O−O	118.2 (121.5)	n/a	74.2	74.4	74.1
∠O−Ti−Cl	95.36 (97.31)	101.4	n/a	n/a	n/a
∠O−O−R	108.8 (107.7)	n/a	102.7	109.4	113.5
∠Ti−O−O−R[d]	157.9 (156.6)	n/a	−113.6	−131.9	−148.2
twist angle[e]	n/a	n/a	3.4	7.2	11.7

[a] Solid-state values from X-ray crystallography in parentheses. [b] UB3LYP. [c] Distance to Cp centroid. [d] Torsion angle. [e] Deviation from orthogonality between the $Cp^#$−Ti−$Cp^#$ plane ($Cp^# = Cp$ centroid) and the O(1)−Ti−O(2) plane for η^2-bound peroxides (see Figure 5).

IV. Computational Studies. $Cp_2Ti(OO^tBu)Cl$ (**1**), its homolysis to [$Cp_2Ti(O^•)Cl + {}^tBuO^•$], and several [$Cp_2Ti(OOR)^+$] cations (R = H, Me, ^{t}Bu) have been studied at the B3LYP level of density functional theory (DFT), with the 6-31G* basis set. Selected metrical data from computed gas-phase structures are given in Table 5 (see Supporting Information for complete details and for computations using the LANL2DZ basis set, which give results similar to those using the 6-31G* basis set). There is very good agreement between the calculated structure of **1** and that observed in the solid state. The largest discrepancy in a bond length is between the calculated Ti−O distance, being 0.03 Å shorter than that found in the X-ray structure. The calculated gas-phase enthalpy for O−O bond homolysis in **1** is 21.6 kcal mol^{-1}. This is a lower limit to the enthalpic barrier and is therefore in good agreement with the experimental solution value $\Delta H^‡ = 24 \pm 2$ kcal mol^{-1}. The calculations are discussed in more detail below.

Discussion

Given the broad interest in peroxide complexes, and titanium peroxide complexes specifically, it is surprising that few examples have been isolated and studied in detail.[1,2,4,13,14] In this work, a series of titanocene *tert*-butylperoxide complexes have been prepared starting from Cp_2TiCl_2 and $NaOO^tBu$ (Scheme 1). With well-characterized materials in hand, we have been able to probe the mechanisms of decomposition and various reactions.

I. Pathway for Decomposition of Peroxide Complexes: O−O Bond Homolysis. The formation of the mixed phosphinites (Et_2PO^tBu from Et_3P, $^nBu_2PO^tBu$ from $^nBu_3P$, and $(PhO)_2PO^tBu$ from $(PhO)_3P$) are to our knowledge unprecedented reactions of metal alkylperoxo complexes. Typically, peroxo species rapidly oxidize phosphines and phosphites to phosphine oxides and phosphates, respectively.[1] The only reasonable way to form R_2PO^tBu compounds in these reactions is via phosphine trapping of the *tert*-butoxyl radical. $^tBuO^•$ adds to Et_3P and other phosphines at close to the diffusion limit to form metastable phosphoranyl radicals [R_3PO^tBu]. The radical from Et_3P decomposes on the millisecond time scale by α-scission (α to the radical center), forming the phosphinite and Et$^•$ (eqs 11, 12).[32] α-Scission is the only observed pathway for [Et_3PO^tBu], even though the alternative *β*-scission to give Et_3PO and $^tBu^•$ is much more thermodynamically favorable.

$$PEt_3 + {}^tBuO^• \xrightarrow{k_{trap} = 1.2 \times 10^9\ M^{-1}\ s^{-1}} [Et_3P^•O^tBu] \quad (11)$$

$$[Et_3PO^tBu] \xrightarrow{k_{\alpha-scission} \sim 10^4\ s^{-1}} Et_2PO^tBu + Et^• \quad (12)$$

Addition of $^tBuO^•$ to Ph_3P, however, is known to proceed by *β*-scission in [Ph_3PO^tBu] to give the phosphine oxide Ph_3PO. Presumably the greater strength of the Ph−P bond disfavors α-scission.[32] $^nBu_3P$ reacts with $^tBuO^•$ to give 80% $^nBu_2PO^tBu$ and 20% $^nBu_3PO$,[33] and $(PhO)_3P + {}^tBuO^•$ gives solely $(PhO)_2PO^tBu$.[34] In each case, these products from $^tBuO^•$ quantitatively match the products observed on reaction of **1** with the respective R_3P. Unfortunately, no products resulting from the ethyl radical (eq 12), such as ethane or chloroethane, were detected in the ^{1}H NMR spectra of reaction mixtures. Thus the reactions of **1** with R_3P involve $^tBuO^•$ as the active oxidant; **1** does not oxidize the phosphines directly.[29] The formation of Et_2PO^tBu in reactions of **3** and **5** with Et_3P indicates a similar pathway in these cases. It should be noted that $^tBuOO^•$ is not involved in the reactions of **1** since this peroxyl radical is known to quantitatively oxidize $(PhO)_3P$ to the phosphate $(PhO)_3PO$,[35] which is not observed. $^tBuOO^•$ in principle could be formed by Ti−O bond homolysis, as reported recently for $Cp_2Ti(TEMPO)(Cl)$.[36]

As a further test for the intermediacy of $^tBuO^•$, reactions of **1** with Ph_3P were run in the presence of tri-*n*-butyl tin hydride. $^nBu_3SnH$ reduces $^tBuO^•$ to ^tBuOH with a rate constant of 2.2×10^8 M^{-1} s^{-1},[37] almost an order of magnitude slower than the rate constant for $Ph_3P + {}^tBuO^•$ (1.9×10^9 M^{-1} s^{-1}).[32] Reaction of **1** + Ph_3P + 20 $^nBu_3SnH$ yields 23% Ph_3PO, as compared to 98% in the absence of $^nBu_3SnH$, and the amount of ^tBuOH increases from 24% to 72% (Table 4). Consistent with the known rate constants, the $^tBuO^•$ is trapped mostly, but not completely, by the 20-fold excess of $^nBu_3SnH$ over the Ph_3P. The changes are not due to any direct reaction of **1** and $^nBu_3SnH$, as the decay of **1** is actually decelerated by the addition of the 20 equiv of $^nBu_3SnH$ (Table 4).

tert-Butoxyl radicals are reduced by Ph_3P to give $^tBu^-$.[32a] $^tBu^•$ can form ^tBuCl by abstracting Cl$^•$—from the CD_2Cl_2 solvent, **1**, Cp_2TiCl_2, and/or other titanium products—or can form isobutylene by donating a H$^•$ to some mild oxidant in the solution ($^tBu^•$ has very weak C−H bonds). ^{t}BuCl and isobutylene

(32) (a) $k_{PR3+tBuO•} = 1.2$ and 1.9×10^9 M^{-1} s^{-1} for Et_3P and Ph_3P, respectively: Griller, D.; Ingold, K. U.; Patterson, L. K.; Scaiano, J. C.; Small, R. D., Jr. *J. Am. Chem. Soc.* **1979**, *101*, 3780−3785. (b) Davies, A. G.; Dennis, R. W.; Griller, D.; Roberts, B. P. *J. Organomet. Chem.* **1972**, *40*, C33−C35.

(33) Chatgilialoglu, C.; Ingold, K. U.; Scaiano, J. C. *J. Am. Chem. Soc.* **1981**, *103*, 7739−7742.

(34) Kochi, J. K.; Krusic, P. J. *J. Am. Chem. Soc.* **1969**, *91*, 3944−39466.

(35) Pobedimskii, D. G.; Kirpichnikov, P. A. *J. Polym. Sci., Polym. Chem. Ed.* **1980**, *18*, 815−825.

(36) (a) Huang, K. W.; Waymouth, R. M. *J. Am. Chem. Soc.* **2002**, *124*, 8200−8201. (b) Huang, K. W.; Han, J. H.; Cole, A. P.; Musgrave, C. B.; Waymouth, R. M. *J. Am. Chem. Soc.* **2005**, *127*, 3807−3816.

(37) Scaiano, J. C. *J. Am. Chem. Soc.* **1980**, *102*, 5399−5400.

Scheme 1. Synthetic Routes to Complexes 2−5 from 1

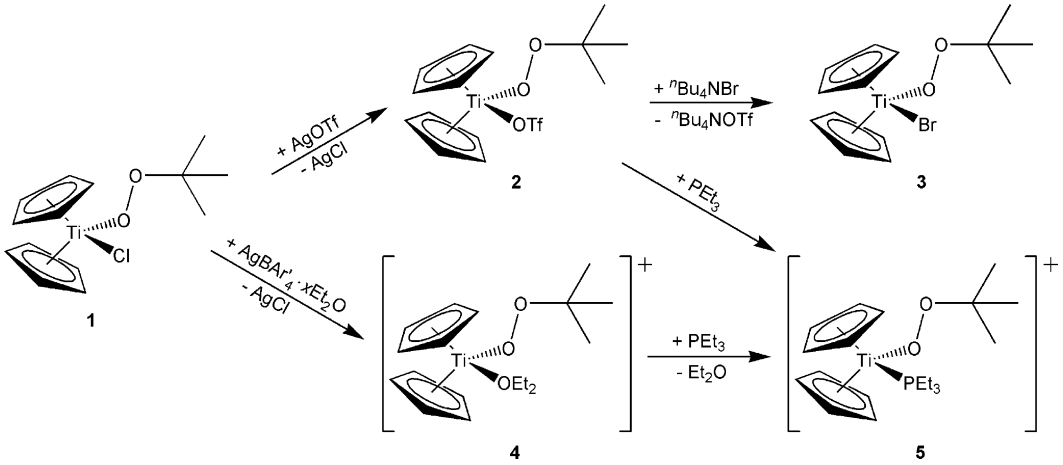

Scheme 2. Mechanism for the Decomposition of Cp$_2$Ti^{IV}(OO^{t}Bu)L in the Presence of Et$_3$P or Ph$_3$P

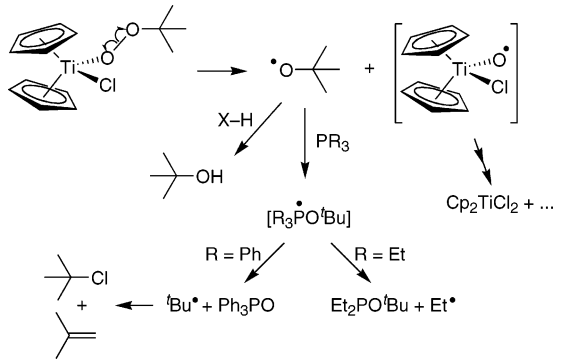

are the dominant C_4 products observed from **1** + Ph_3P (Table 4). In the absence of phosphines, the ^{t}BuO$^•$ abstracts hydrogen from solvent or some other source to give high yields of ^{t}BuOH/^{t}BuOD. Apparently, this abstraction is faster than decomposition of ^{t}BuO$^•$ to acetone, as none of this product is observed.[38] The 24% yield of ^{t}BuOH in the presence of Ph_3P likely results not from this H atom abstraction pathway, but rather from oxidation of ^{t}Bu$^•$ by **1** or some other species. In the presence of Et_3P, the ^{t}Bu groups are retained in the Et_2PO^tBu product and very low yields of ^{t}BuOH, ^{t}BuCl, and $CH_2{=}CMe_2$ are found.

The data all indicate the presence of ^{t}BuO$^•$ as the primary oxidant, formed by homolytic cleavage of the O−O bond (Scheme 2). Unimolecular O−O bond homolysis is the rate-limiting step, as the rate constants for decomposition (k_{dec}) with various added substrates over a range of concentrations vary by less than a factor of 2 (Table 4). The variation in k_{dec} is likely due to changes in the stoichiometry of decomposition. For instance, if the ^{t}Bu$^•$ radical generated from **1** in the presence of Ph_3P itself consumes 1 equiv of **1**, then the observed rate constant for the decay of **1** would be twice the rate of homolysis. Rate-limiting homolysis is further supported by the small positive $\Delta S^‡$ values for the decompositions of **1**, **3**, **4**, and **5** (Table 3). A radical chain mechanism is not likely because of the reproducible simple first-order kinetic behavior and because the decomposition of **1** is little affected by the oxidative and reductive radical traps CBr_4 and ^{n}Bu$_3$SnH (Table 4). The ease of homolysis in **1** is consistent with the tentatively assigned O−O stretching frequency, 819 cm^{-1}, since this is significantly lower than ν(OO) in ^{t}BuOO^{t}Bu (920 cm^{-1} [39]). Structural parameters, however, do not show much difference in **1** versus ^{t}BuOO^{t}Bu, either in the O−O distance (1.467(2) versus 1.478(3) Å) or the X−O−O−C torsion angle (156.6(1)° versus 164.1(7)°).[40] The DFT-calculated gas-phase enthalpy for O−O bond homolysis in **1** of 21.6 kcal mol^{-1} is also consistent with the experimental enthalpic barrier in solution of 24 ± 2 kcal mol^{-1}. This barrier to homolysis is 10 kcal mol^{-1} lower than the 34 kcal mol^{-1} determined for ^{t}BuOO^{t}Bu and 16−19 kcal mol^{-1} lower than organic hydroperoxides, which typically have a bond strength of 40−43 kcal mol^{-1}.[1b]

O−O bond homolysis is a common mode of decomposition of metal alkylperoxide complexes, as in the Haber-Weiss mechanism (and the Fenton reaction for $Fe^{2+} + H_2O_2$).[1,6a] Que and co-workers have generated Fe(TPA)(OO^{t}Bu) at low temperature and determined that it undergoes homolysis to ^{t}BuO$^•$ and an iron(IV)-oxo intermediate (TPA = tris(2-pyridylmethyl)-amine).[41] A series of cobalt(III) alkylperoxide complexes have been prepared by Mascharak et al. and shown to undergo homolysis upon mild heating.[42] In contrast, the copper(II) *tert*-butylperoxide complex Cu(OO^{t}Bu)(HB(3-^{t}Bu-5-^{i}Prpz)$_3$) does not appear to undergo homolysis (which is calculated to have a high barrier) but rather acts as an electrophilic oxidant.[43] The only previous examples of d^0 peroxide complexes undergoing homolysis are the hafnocene derivatives Cp*$_2$Hf(OO^{t}Bu)Cl and Cp*$_2$Hf(OO^{t}Bu)(C$_6$H$_5$) reported by Bercaw et al.[9] In the presence of 9,10-dihydroanthracene, the latter compound converts to Cp*$_2$Hf(C$_6$H$_5$)OH and ^{t}BuOH.[9] The barrier for homolysis in Cp*$_2$Hf(OO^{t}Bu)Cl is $\Delta H^‡$ = 22.6 kcal mol^{-1}, similar to what is seen for **1**−**5**.

Homolyses of the O−O bonds in Cp$_2$Ti^{IV}(OO^{t}Bu)L (**1**−**5**) and Cp*$_2$Hf^{IV}(OO^{t}Bu)L are surprising because, unlike the cases above, the oxyl-metal product cannot be stabilized by oxidation of the metal center. Homolysis of **1** generates ^{t}BuO$^•$ and a titanyl species "Cp$_2$Ti(O$^•$)Cl", following eq 5 above. While the fate of

(38) The fate of ^{t}BuO$^•$ in methylene chloride with added cyclohexane (as a H$^•$ source) has been documented: Russell, G. A. *J. Org. Chem.* **1959**, *24*, 300−302.

(39) Vacque, V.; Sombret, B.; Huvenne, J. P.; Legrand, P.; Suc, S. *Spectrochim. Acta, Part A* **1997**, *53*, 55−66.

(40) Slovokhotov, Y. L.; Timofeeva, T. V.; Antipin, M. Y.; Struchkov, Y. T. *J. Mol. Struct.* **1984**, *112*, 127.

(41) (a) Zang, Y.; Kim, J.; Dong, Y.; Wilkinson, E. C.; Appelman, E. H.; Que, L., Jr. *J. Am. Chem. Soc.* **1997**, *119*, 4197−4205. (b) Lehnert, N.; Ho, R. Y. N.; Que, L., Jr.; Solomon, E. I. *J. Am. Chem. Soc.* **2001**, *123*, 8271−8290.

(42) (a) Chavez, F. A.; Nguyen, C. V.; Olmstead, M. M.; Mascharak, P. K. *Inorg. Chem.* **1996**, *35*, 6282−6291. (b) Chavez, F. A.; Briones, J. A.; Olmstead, M. M.; Mascharak, P. K. *Inorg. Chem.* **1999**, *38*, 1603−1608. (c) Chavez, F. A.; Mascharak, P. K. *Acc. Chem. Res.* **2000**, *33*, 539−545.

(43) Chen, P.; Fujisawa, K.; Solomon, E. I. *J. Am. Chem. Soc.* **2000**, *122*, 10177−10193, and references therein.

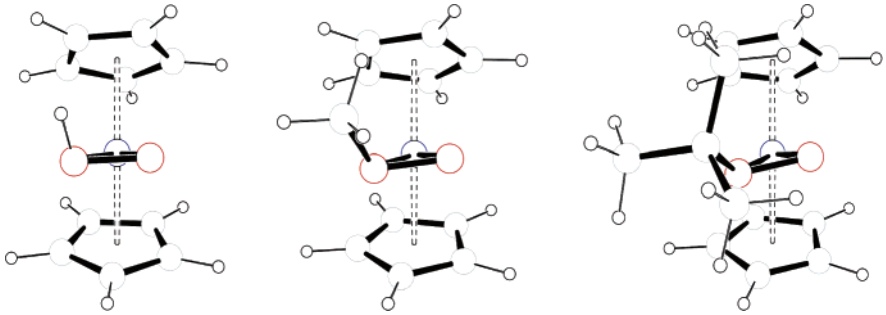

Figure 3. Geometry optimizations for [$Cp_2Ti(\eta^2$-OOR)$^+$], R = H, Me, and ^{t}Bu (B3LYP/6-31G*).

the *tert*-butoxyl radical is amply documented (see above), there is essentially no experimental information about the titanyl radical product $Cp_2Ti(O^\bullet)Cl$. The titanyl might have been expected to add to olefins, to transfer its oxygen atom to Et_3P to form Et_3PO, or to be trapped by $^n Bu_3SnH$, but these are not observed. This contrasts with the trapping of putative "Cp^*_2-Hf($O^\bullet$)Cl" by 9,10-dihydroanthracene to give the hydroxide.[9] It is possible that $Cp_2Ti(O^\bullet)Cl$ is highly reactive and is rapidly converted to a myriad of products, making it difficult to trap with external reagents.

The nature of the implicated titanyl intermediate, $Cp_2Ti(O^\bullet)$-Cl, has been probed by DFT calculations using the UB3LYP functional (Table 5). The computed Ti−O distance of 1.699 Å is 0.18 Å shorter than the Ti−O bond in **1** and is a reasonable value for a "normal" titanyl (L_nTi^{IV}=O) complex. Cp^*_2Ti(=O)-(4-phenylpyridine), for instance, has d(Ti=O) = 1.665(3) Å, as measured by X-ray crystallography.[44] This suggests the presence of some Ti−O π bonding in $Cp_2Ti(O^\bullet)Cl$, although no specific π-bonding orbital is evident in the valence MOs. The Mulliken atomic spin populations (α spin−β spin; see Supporting Information) indicate that the oxyl oxygen carries the largest spin density (0.58), followed by the titanium (0.22) and four of the Cp carbon atoms (0.12−0.19). These four carbon atoms are close to the Ti−O π orbital perpendicular to the Ti−O−Cl plane, and such an interaction may be responsible for their spin densities. The Ti−Cp interaction in $Cp_2Ti(O^\bullet)Cl$ appears to be perturbed relative to **1**, based on the ∼0.03 Å increase in the Ti−Cp(centroid) distances (although as above this is not evident from the valence MOs). In sum, the calculations suggest that the putative titanyl intermediate could be described as a mixture of resonance structures $Cp_2Ti(O^\bullet)Cl$ and ($Cp^\bullet$)(Cp)Ti(=O)(Cl).

II. Attempted Conversion to η^2-Alkylperoxide Complexes: The Limited Reactivity of 1−5. Compounds **1**−**5** are remarkably inert toward oxygen atom transfer for a peroxide complex, particularly as a complex of a Lewis-acidic, early transition metal. We attribute this lack of reactivity to the η^1 coordination mode of the alkylperoxide ligand. These compounds all have a 16-electron count—considering the peroxide as a σ-only ligand—and could in principle convert to an η^2 structure without ligand loss. Instead, they approach an 18e^- configuration through π-donation from the peroxide α oxygen, as indicated by the short Ti−O distances and the orientation of the η^1 peroxide ligand. Removal of the chloride ligand in **1** does not form a cationic η^2 complex: even the weak ligands triflate and Et_2O bind to the titanium centers in **2** and **4** in preference to an η^2 complex.

η^2 Complexes of ^{t}BuOO$^-$ are thought to be common intermediates in reactions mediated by compounds of titanium and other early metals,[1−5] so there must be some feature(s) specific to the metallocene structure that disfavor η^2-coordination. Electronically, η^2-coordination prevents π-donation from the peroxide ligand because the frontier orbitals of the bent metallocene are localized in the "wedge" plane.[19] Thus a species such as [$Cp_2Ti(\eta^2$-OOR)$^+$] could only achieve a 16e^- configuration. Perhaps more important is the unfavorable steric interaction between the Cp ligands and the ^{t}Bu substituent in [$Cp_2Ti(\eta^2$-OO^{t}Bu)$^+$]. This steric clash is indicated by the DFT-calculated structures for [$Cp_2Ti(\eta^2$-OOR)]$^+$ with R = H, Me, and ^{t}Bu. The optimized geometries (Figure 3, Table 5) show increasing distortions of the peroxide ligand with increasing steric bulk of the R group. The peroxide twists out of the equatorial plane of the metallocene: the deviations from orthogonality between the O−Ti−O and $Cp^\#$−Ti−$Cp^\#$ planes ($Cp^\#$ = Cp centroid) are 3.4°, 7.2°, and 11.7° for R = H, Me, and ^{t}Bu, respectively. In addition, the R group is pushed away from the metal, with increasing Ti−O−O−R torsion angles of 114°, 132°, and 148°. Remarkably, the η^2-form [$Cp_2Ti(\eta^2$-OO^{t}Bu)]$^+$ is calculated to be 1 kcal mol^{-1} higher in enthalpy than the unsaturated [$Cp_2Ti(\eta^1$-OO^{t}Bu)]$^+$ isomer. This is consistent with even very weak ligands giving [$Cp_2Ti(\eta^1$-OO^{t}Bu)(L)]$^{+/0}$ rather than an η^2 form. In essence, the bulk of the ^{t}Bu group prevents the formation of the η^2 isomer. In light of this, catalytic systems using titanocene dichloride and ^{t}BuOOH seem likely to involve cleavage of a Cp ring to allow for η^2-coordination and the resulting reactivity observed.[12,15]

Conclusions

A series of titanocene complexes with η^1-*tert*-butylperoxide ligands, $Cp_2Ti^{IV}(\eta^1$-OO^{t}Bu)L, have been prepared [L = Cl (**1**), OTf (**2**), Br (**3**), Et_2O (**4**), PEt_3 (**5**)]. Compounds **1**−**5** all decompose at ambient temperature, and phosphine-trapping studies indicate a mechanism of O−O bond homolysis for **1**, **3**, and **5**. Homolysis generates ^{t}BuO$^\bullet$, which reacts with Et_3P to give Et_2PO^tBu. Facile O−O homolysis is surprising since the titanium(IV) centers are d^0 and cannot be oxidized; peroxide bond homolyses in transition metal complexes typically are facilitated by concomitant oxidation of the metal. Compounds **1**−**5** do not oxidize alkenes or phosphines, which was unexpected in light of the wide use of titanium compounds as catalysts for oxidations where peroxides are the terminal oxidants. Homolysis and the lack of direct oxygen atom reactivity in **1**−**5** are likely due to the inability of the complexes to form more reactive η^2 conformers, apparently for steric reasons.

Experimental Section

General Procedures. All manipulations were performed under an argon or nitrogen atmosphere, using standard high-vacuum-line

(44) Smith, M. R.; Matsunaga, P. T.; Andersen, R. A. *J. Am. Chem. Soc.* **1993**, *115*, 7049−7050.

or inert atmosphere glovebox techniques unless otherwise noted. All glassware was flame-dried under vacuum immediately before use. Protio (Fisher Scientific) and deuterio solvents (Cambridge Isotope) were dried and degassed over Na/Ph_2CO (pentane, cyclohexane, hexanes, benzene, toluene, Et_2O, THF) or CaH_2 (CH_2Cl_2) and vacuum transferred immediately before use. Cp_2TiCl_2 (99+%) and AgOTf (99%) (both Strem) were used as received. $AgBAr'_4 \cdot xEt_2O$ was synthesized following literature procedures.[25] $^nBu_4NBr$ (Aldrich) was ground finely in a mortar and pestle and dried under vacuum. Following a related procedure,[45] $NaOO^tBu$ was synthesized by precipitation from equimolar amounts of HOO^tBu (~5.5 M in decane over 4 Å molecular sieves, >97%) and NaO^tBu (>97%, both from Fluka) in THF, filtered, dried in vacuo, and stored in a desiccator.

NMR spectra were obtained at 300 K (unless otherwise noted) on Bruker Avance DRX-499, AV-500, or DMX-750 spectrometers. NMR spectra were obtained using either J. Young-valved sealable or flame-sealed NMR tubes and are referenced to residual solvent peaks for ^1H and ^{13}C, external 85% H_3PO_4 (in a sealed capillary) for ^{31}P, or external $CFCl_3$ for ^{19}F. Mass spectra were performed in EI^+ ionization mode using a direct inlet probe (hot stage) on Kratos Profile HV-3 (low-resolution) or JEOL HX-110 (high-resolution) mass spectrometers. FT-IR spectra were obtained on a Bruker VECTOR 22/N-C spectrophotometer using a NaCl solution cell. Elemental analyses were performed by Atlantic Microlab (Norcross, GA).

CAUTION: All the metal peroxide complexes described here should be prepared and handled in small quantities, stored in an inert atmosphere below 0 °C, and manipulated with Teflon-coated spatulas. Complex **1** has been observed to undergo spontaneous exothermic decomposition in the solid state.

$Cp_2Ti(OO^tBu)Cl$ (1). In the air, Cp_2TiCl_2 (100 mg, 0.40 mmol) and $NaOO^tBu$ (180 mg, 1.60 mmol) were ground together carefully using a mortar and pestle. The mixed solids were placed in a swivel-frit assembly and evacuated on a vacuum line. THF (50 mL) was vacuum transferred onto the solids at −78 °C, and the reaction mixture was stirred at −20 °C for 2 h. The THF was removed in vacuo at ambient temperature and hexanes (50 mL) vacuum transferred in. The resulting solids were filtered and washed with excess hexanes until the filtrate was no longer yellow in color. Removal of the hexanes, addition of 10 mL of pentane, and filtration gave yellow **1** (102 mg, 84%). X-ray quality crystals were obtained by cooling a saturated, filtered toluene solution of **1** at −5 °C for 24 h. ^1H NMR (THF-d_8, −20 °C): 6.35 (s, 10H, C_5H_5), 1.09 (s, 9H, $C(CH_3)_3$). $^{13}C\{^1H\}$ NMR (THF-d_8, −20 °C): 117.3 (s, C_5H_5), 82.4 (s, $OOCMe_3$), 27.0 (s, $OOC(CH_3)_3$). IR (CH_2Cl_2, cm^{-1}): 3008 s (CH); 1451 s, 1445 s, 1206 s (^{t}Bu); 1018 w (CO); 815 m (OO). MS for $^{12}C_{14}{}^1H_{19}{}^{35}Cl^{16}O_2{}^{48}Ti$ (M^+): calcd, 302.05530; found, 302.05544. Anal. Calcd for $C_{14}H_{19}ClO_2Ti$: C, 55.62; H, 6.34. Found: C, 55.71; H, 6.33.

$Cp_2Ti(OO^tBu)OTf$ (2). THF (25 mL) was vacuum transferred onto **1** (100 mg, 0.33 mmol) and AgOTf (85 mg, 0.33 mmol) at −78 °C, and the reaction mixture was stirred at −20 °C for 2 h. The THF was removed in vacuo at 0 °C, and Et_2O (50 mL) was added. The suspension was stirred at −20 °C for 0.5 h and filtered at −78 °C to remove the AgCl and any residual AgOTf, and immediately the Et_2O was removed in vacuo at −20 °C, yielding **2** as an orange solid. Complex **2** is unstable at temperatures over 0 °C, decomposing quickly both in solution and as a solid. ^1H NMR (THF-d_8, −20 °C): 6.58 (s, 10H, C_5H_5), 1.17 (s, 9H, $C(CH_3)_3$). $^{13}C\{^1H\}$ NMR (THF-d_8, −20 °C): 120.4 (q, J_{C-F} = 318 Hz, OSO_2CF_3), 118.8 (s, C_5H_5), 83.6 (s,$OOCMe_3$), 26.7 (s, $OOC(CH_3)_3$). ^{19}F NMR (THF-d_8, −20 °C): 79.2 (s, OSO_2CF_3).

$Cp_2Ti(OO^tBu)Br$ (3). Complex **2** was generated as above, quickly dissolved in THF (25 mL), and at −78 °C $^nBu_4NBr$ (106 mg, 0.33 mmol) was added. The reaction mixture was stirred at −20 °C for 2 h, and the THF was removed in vacuo at ambient temperature. Et_2O (25 mL) was added, and the resulting solids were filtered and washed with excess Et_2O until the filtrate was no longer yellow. The volume of Et_2O was reduced to ~5 mL, and pentane (5 mL) was added, yielding 71 mg of yellow **3** (62% based on **1**). X-ray quality crystals were obtained by the slow evaporation of a saturated CH_2Cl_2 solution of **3** at −5 °C for 48 h. ^1H NMR (THF-d_8, −20 °C): 6.40 (s, 10H, C_5H_5), 1.08 (s, 9H, $C(CH_3)_3$). $^{13}C\{^1H\}$ NMR (THF-d_8, −20 °C): 117.1 (s, C_5H_5), 82.7 (s,$OOCMe_3$), 27.0 (s, $OOC(CH_3)_3$). IR (CH_2Cl_2, cm^{-1}): 2985 m (CH); 1449 w, 1361 w, 1188 w (^{t}Bu); 1016 w (CO); 819 m (OO). MS for $^{12}C_{14}{}^1H_{19}{}^{79}Br^{16}O_2{}^{48}Ti$ (M^+): calcd, 346.00478; found, 346.00486. Anal. Calcd for $C_{14}H_{19}BrO_2Ti$: C, 48.45; H, 5.52. Found: C, 48.23; H, 5.48.

$[Cp_2Ti(OO^tBu)OEt_2][BAr'_4]$ (4). An NMR tube was charged with 10.0 mg (0.033 mmol) of **1** and 36.9 mg (0.033 mmol) of $AgBAr'_4 \cdot 2Et_2O$, and ~0.7 mL of CD_2Cl_2 was vacuum transferred in at low temperature. The NMR tube was sealed and, keeping it at or below −20 °C, shaken thoroughly and then placed vertically for 30 min to allow the AgCl to settle. ^1H NMR (CD_2Cl_2, −20 °C): 7.73 (br s, 8H, *o*-Ar′), 7.58 (s, 4H, *p*-Ar′), 6.51 (s, 10H, C_5H_5), 3.61 (br q, 4H, $^3J_{HH}$ = 7 Hz, $O(CH_2CH_3)_2$), 1.29 (t, 6H, $^3J_{HH}$ = 7 Hz, $O(CH_2CH_3)_2$), 1.16 (s, 9H, $C(CH_3)_3$). $^{13}C\{^1H\}$ NMR (CD_2Cl_2, −20 °C): 161.5 (q, J_{C-B} = 50 Hz, B-*ipso*-Ar′), 134.8 (s, *o*-Ar′), 129.0 (qq, J_{C-F} = 32, 3 Hz, *m*-Ar′), 124.8 (q, J_{C-F} = 272 Hz, CF_3), 118.6 (s, *p*-Ar′), 117.8 (s, C_5H_5), 85.0 (s, $OOCMe_3$), 66.8 (s, Ti-$O(CH_2CH_3)_2$), 26.1 (s, $OOC(CH_3)_3$), 15.7 (br s, Ti-$O(CH_2CH_3)_2$).

$[Cp_2Ti(OO^tBu)Et_3P][BAr'_4]$ (5). Complex **4** was prepared as above except that the reaction was run in the glovebox freezer in a 1 dram vial with the reagents, solvent, and apparatus precooled to −20 °C. CD_2Cl_2 (~0.7 mL) was added to the solids, and the reaction was mixed and after 10 min filtered through two 13 mm nylon-membrane syringe filters (0.45 μm pore size, Gelman Acrodisc) using a 1 mL glass syringe. The filtrate was injected into a J. Young-valved sealable NMR tube containing Et_3P (5 μL, 0.033 mmol) at −20 °C. ^1H NMR (CD_2Cl_2, −20 °C): 7.73 (br s, 8H, *o*-Ar′), 7.58 (s, 4H, *p*-Ar′), 6.27 (d, J_{H-P} = 3 Hz, 10H, C_5H_5), 1.96 (br m, 6H, $P(CH_2CH_3)_3$), 1.10 (dt, J_{H-P} = 7 Hz, J_{H-H} = 8 Hz, 9H, $P(CH_2CH_3)_3$), 1.16 (s, 9H, $C(CH_3)_3$). $^{13}C\{^1H\}$ NMR (CD_2Cl_2, −20 °C): 162.0 (q, J_{C-B} = 50 Hz, B-*ipso*-Ar′), 135.0 (s, *o*-Ar′), 129.0 (qq, J_{C-F} = 31, 3 Hz, *m*-Ar′), 124.8 (q, J_{C-F} = 272 Hz, CF_3), 117.8 (s, *p*-Ar′), 115.6 (d, J_{C-P} = 4 Hz, C_5H_5), 85.0 (s, $OOCMe_3$), 26.0 (s, $OOC(CH_3)_3$), 17.3 (d, J_{C-P} = 13 Hz, $P(CH_2CH_3)_3$), 9.0 (br s, $P(CH_2CH_3)_3$). $^{31}P\{^1H\}$ NMR (CD_2Cl_2, −20 °C): 27.6 (s).

Et_2PO^tBu. Et_2PCl (100 mg, 0.80 mmol, Acros Organics) was added to a stirring solution of Et_3N (809 mg, 8.00 mmol) and ^{t}BuOH (593 mg, 8.00 mmol) in dry benzene (10 mL). After stirring overnight, a white precipitate (presumably Et_3NHCl) was filtered off, and the volatiles were removed in vacuo, leaving Et_2PO^tBu as a thick oil. $^{31}P\{^1H\}$ NMR (CD_2Cl_2): 109.6 ppm. MS: 162 *m*/*z*.

^1H NMR Kinetics. In a typical reaction, a vial was charged with **1** (10.0 mg, 0.033 mmol), C_6Me_6 (1.0 mg) as an internal standard, and Ph_3P (8.7 mg, 0.033 mmol). CD_2Cl_2 (0.5 mL) was added, and the resulting solution was rapidly transferred to a J. Young-valved sealable NMR tube, sealed, and quickly frozen in liquid N_2. The NMR tube was warmed to room temperature at the spectrometer, and spectra were acquired every 5 min for at least 3 h, employing a 10 s delay between pulses for accurate integration. Peaks in each spectrum were integrated individually versus the internal standard and the residual solvent peak using WinNuts.

X-ray Crystallographic Studies. Crystals were mounted on a glass capillary with oil at −143 °C. Intensity data were collected on an Enraf-Nonius KappaCCD diffractometer equipped with a fine focus Mo-target X-ray tube. The data were integrated and scaled using hkl-SCALEPACK (hkl-2000 for **3**).[46] These programs apply

(45) NaOEt + $HOO^tBu \rightarrow NaOO^tBu$: Lobanova, G. N. *Visn. L'viv. Politekh. Inst.* **1971**, *58*, 11−14.

a multiplicative correction factor (S) to the observed intensities (I): $(e^{-2B(\sin^2\theta)/\lambda^2})$/scale. S is calculated from the scale and the B factor, which is determined for each frame and is then applied to I to give the corrected intensity (I_{corr}). Solution by direct methods (SIR 97) produced a complete heavy atom-phasing model.[47] All hydrogen atoms were placed using a riding model. All non-hydrogen atoms were refined anisotropically by full-matrix least squares (SHELXL-97, Table 2).[48]

Computational Studies. Geometries were optimized and vibrational analyses were performed at the density functional (DFT) level of theory using the 6-31G* basis set.[49] The hybrid B3LYP functional was employed, which combines Becke's gradient-corrected exchange functional[50] with the gradient-corrected correlation functional of Lee, Yang, and Parr.[51] The vibrational analyses were used to confirm the nature of the stationary points, and the unscaled vibrational frequencies were used to compute thermal contributions to enthalpies. All of the calculations were carried out with the Gaussian 03 suite of programs.[52]

Acknowledgment. We are grateful to the U.S. National Institutes of Health (grant R01 GM50422 to J.M.M.) and the U.S. National Science Foundation (grant CHE-0239304 to W. T. Borden) for support of this work.

Supporting Information Available: Metrical data for DFT-calculated structures and intermediates, Eyring plots for the decomposition of **1** and **3**−**5** in CD_2Cl_2, and CIF files for **1** and **3**. This material is available free of charge via the Internet at http://pubs.acs.org.

OM050818Z

(46) Otinowski, Z.; Minor, W. Processing of X-ray Diffraction Data Collected in Oscillation Mode. In *Methods in Enzymology*; Carter, C. W., Jr., Sweet, R. M., Eds.; Academic Press: New York, 1996; pp 307−326.

(47) Altomare, A.; Cascarano, G.; Giacovazzo, C.; Burla, M. C.; Polidori, G.; Camalli, M. *J. Appl. Crystallogr.* **1994**, *27*, 435−442.

(48) Sheldrick, G. M. *SHELXL-97: Program for the Refinement of Crystal Structures*; University of Göttingen: Göttingen, Germany, 1997.

(49) Hariharan, P. C.; Pople, J. A. *Theor. Chim. Acta* **1973**, *28*, 213−222.

(50) Becke, A. D. *J. Chem. Phys.* **1993**, *98*, 5648−5652.

(51) Lee, C.; Yang, W.; Parr, R. G. *Phys. Rev. B* **1988**, *37*, 785−789.

(52) Frisch, M. J.; Trucks, G. W.; Schlegel, H. B.; Scuseria, G. E.; Robb, M. A.; Cheeseman, J. R.; Montgomery, J. A., Jr.; Vreven, T.; Kudin, K. N.; Burant, J. C.; Millam, J. M.; Iyengar, S. S.; Tomasi, J.; Barone, V.; Mennucci, B.; Cossi, M.; Scalmani, G.; Rega, N.; Petersson, G. A.; Nakatsuji, H.; Hada, M.; Ehara, M.; Toyota, K.; Fukuda, R.; Hasegawa, J.; Ishida, M.; Nakajima, T.; Honda, Y.; Kitao, O.; Nakai, H.; Klene, M.; Li, X.; Knox, J. E.; Hratchian, H. P.; Cross, J. B.; Bakken, V.; Adamo, C.; Jaramillo, J.; Gomperts, R.; Stratmann, R. E.; Yazyev, O.; Austin, A. J.; Cammi, R.; Pomelli, C.; Ochterski, J. W.; Ayala, P. Y.; Morokuma, K.; Voth, G. A.; Salvador, P.; Dannenberg, J. J.; Zakrzewski, V. G.; Dapprich, S.; Daniels, A. D.; Strain, M. C.; Farkas, O.; Malick, D. K.; Rabuck, A. D.; Raghavachari, K.; Foresman, J. B.; Ortiz, J. V.; Cui, Q.; Baboul, A. G.; Clifford, S.; Cioslowski, J.; Stefanov, B. B.; Liu, G.; Liashenko, A.; Piskorz, P.; Komaromi, I.; Martin, R. L.; Fox, D. J.; Keith, T.; Al-Laham, M. A.; Peng, C. Y.; Nanayakkara, A.; Challacombe, M.; Gill, P. M. W.; Johnson, B.; Chen, W.; Wong, M. W.; Gonzalez, C.; Pople, J. A. *Gaussian 03*, Revisions B.05; Gaussian, Inc.: Wallingford, CT, 2004.